International Journal of ChemTech Research
CODEN (USA): IJCRGG ISSN: 0974-4290
Vol.7, No.3, pp 1452-1459, 2014-2015

ICONN 2015 [4th - 6th Feb 2015]
International Conference on Nanoscience and Nanotechnology-2015
SRM University, Chennai, India

Protein capped silver nanoparticles from fungus: X-ray Diffraction Studies with Antimicrobial properties against bacteria

Swarup Roy*, Tapan Kumar Das

Department of Biochemistry and Biophysics, University of Kalyani, Kalyani – 741235, West Bengal, India

Abstract : The present study shows an eco-friendly and low-cost method of biosynthesis of silver nanoparticles (SNP) using live cell-free filtrate of fungus, *Aspergillus foetidus*. Synthesis of SNP has been done by using extracellular cell filtrate of fungus, *Aspergillus foetidus* and 1 mM aqueous solution of silver nitrate. The SNP were characterized by the following different biophysical techniques: UV-Visible spectrum, Dynamic Light Scattering, Zeta potential, Fourier Transform Infrared spectroscopy, Atomic Force Microscopy, Transmission Electron Microscopy, Energy Dispersive X-ray spectrum and nitrate reductase assay. X-ray diffraction (XRD) spectrum of the nanoparticles exhibited 2θ values corresponding to face-centered cubic (FCC) SNP and XRD studies reveal a high degree of crystallinity and monophasic SNP. Their average particle size is found to be 10.59 nm and specific surface area (SSA) is 53.96 m^2/g. The crystallinity index indicates that the silver metal is highly crystalline and FCC phase structure is well-indexed with polycrystalline nature. Scanning Electron Microscope (FESEM)) analysis proved the spherical shape and 10-30 nm size of the particle. Antimicrobial activities of the SNP have been carried out against the growth of both gram positive and gram negative bacteria. The nanoparticles showed inhibitory effect on the growth kinetics of both gram positive and gram negative bacteria.
Key Words: Silver Nanoparticles, Biosynthesis, XRD, FESEM, Antibacterial activity.

Introduction

Silver nanoparticles can be prepared using chemical, physical and biological methods but unlike biological synthesis for chemical and physical methods under high temperature, pressure, chemical solvent and capping agents are required for the preparation of nanoparticles[1]. In case of biologically synthesized nanoparticles microorganisms (bacteria and fungi) and plants are often used for synthesis of ecofriendly nanoparticles both in extracellular and intracellular process[2-5]. T he bioprocess of synthesis of nanomaterials is less laborious, low-cost and most significantly nontoxic, making the biological method advantageous compared with the physical and chemical methods. The biological agents including fungi secrete a large number of enzymes, which played a main role in enzymatic reduction of metals ions as an essential step for synthesis of SNP[6]. In case of fungi, nitrate reductase is found to be responsible for the extracellular biosynthesis of nanoparticles[7-8].

Silver nanoparticles possess antibacterial[9], anti-fungal[10] and anti-cancer activities[11]. Developing SNP as a new generation of antimicrobial agents may be an attractive and cost-effective means to overcome the drug resistance problem seen against Gram-negative and Gram positive bacteria. Now a days nanoscale material have grown up as novel antimicrobial agents owing to their high surface area to volume ratio and its unique chemical and physical properties[12]. Nanotechnology is coming out as a rapidly growing field with its application in science and technology for the purpose of making up new materials at the nanoscale level[13]. Antimicrobial activity of SNP have been studied by various researchers especially on *Escherichia col*i and *Staphylococcus aureus* [14, 15], same strain has been used in the present work to study the antibacterial activity of SNP synthesized from *Aspergillus foetidus*. Silver nanoparticles have been previously synthesized from *Aspergillus foetidus*[16, 17, 18]. This work is mainly focused on the study of X-Ray diffraction analysis of biosynthesized SNP and the antibacterial activity of SNP on *E. coli,* and *S. aureus*.

Experimental:

Materials

Silver nitrate (Merck, Germany), Nutrient agar, and Nutrient broth (SRL, India) were used in this experiment. All the other chemicals were of analytical reagent grade and double distilled water was used throughout.

Methods

Synthesis and Characterization of SNP

Silver nanoparticles have been prepared by using extracellular cell filtrate of fungus *Aspergillus foetidus* and aqueous solution of silver nitrate (1mM). The biosynthesized SNP were characterized by UV-Vis spectra, DLS analysis, Zeta potential measurement, FTIR spectroscopy, AFM, TEM, and EDAX analysis as mentioned in our previous report[16]. After biosynthesis of nanoparticles the process of synthesis has been optimized and the concentration of nanoparticles has been determined as shown in our earlier report[17, 18]. The details of biosynthesis and characterization procedure have been mentioned in our previous report.

X-Ray Diffraction Studies

X-Ray Diffraction analysis of the freeze dried powdered prepared sample of SNP on a glass slide was done using a Rigaku, MiniFlex X-Ray Diffractometer, Cu-Kα X-rays of wavelength (λ) =1.541 Å (Energy-40KV, Current- 30mA) and data was taken for the 2θ range of 20° to 90° with a step size of 0.02°.

SEM analysis of silver nanoparticles

Field emission scanning electron microscopic (FESEM) analysis was done using FESEM- QUANTA FEG 250 instrument. Thin films of the sample were prepared on a silicon waiver by just dropping 10µl of the sample and then the film on the SEM sample was allowed to dry at vacuum condition and sample was analyzed at 5KV energy.

Antibacterial Activity

The antibacterial activity of SNP was evaluated against the strains *E. coli*, and *S. aureus*. Cultures were maintained on LB agar slants and they were sub cultured before use. Fresh overnight cultures of inoculum (100 µl) of each culture were spread on to LB agar plates. Well diffusion method was used to assay in vitro antibacterial activity[19]. Three wells of~ 5mm diameter has been made using gel borer for positive control (antibiotic, 10mg/ml), negative control (salt solution, 1mM) and test solution (SNP, 100µM) in each plate. Samples were placed on the agar well and incubated for 24 h at 37°C. After incubation at 37°C for 24 h, the different levels of zone of inhibition of growth around wells were measured to evaluate the antibacterial activity. Growth curve of both strains has also been studied in presence of SNP.

Results and Discussion

Biosynthesized silver nanoparticles

Green synthesis of nanoparticles has evolved as a cost effective, eco-friendly and a unique alternative to

chemical synthesis. Silver nanoparticles are commonly synthesized by the chemical method using different reducing agent. Due to the toxicity of these chemical agents the alternative eco-friendly biological synthesis methods are formulated which involves enzymatic reduction with better control over size and shape. We prepared SNP by using a fungi *Aspergillus foetidus*. Here an enzyme nitrate reductase released extracellularly is believed to bring about the reduction of Ag^{+} to Ag^{o}. This cost-effective, ecofriendly bio-mediated synthetic process excludes the need of addition of an external capping agent as in this kind of biosynthesis process cellular enzyme or protein act as a capping agent and also essentially provides SNP with high stability. Fig. 1 shows the basic color change of light yellow to brown color during formation of SNP, signature peak of SNP in UV-Vis spectrum at 410 nm, and roughly spherical shaped 20-40nm size image of SNP in transmission electron microscopy.

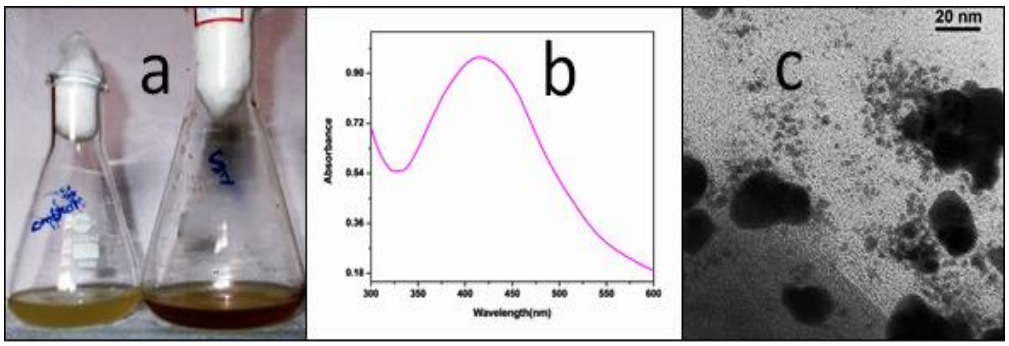

Fig.1 Color Change (light yellow to amber color), UV-Vis Spectrum, and TEM image of biosynthesized silver nanoparticles (a, b, c respectively).

X-Ray Diffraction Studies

Peak Indexing

The X-ray diffraction form of the biosynthesized SNP is shown in Fig.2. A number of strong Bragg reflections can be seen which correspond to the (111), (200), (220), (311) and (222) reflections of FCC silver (Table.1). All the reflections correspond to pure silver metal with face centered cubic symmetry.

The high intense peak for FCC materials is generally (111) reflection, which is observed in the sample. The intensity of peaks reflected the high degree of crystallinity of the SNP. However, the diffraction peaks are broad which indicating that the crystallite size is small[20]. The size of the Ag nanoparticles estimated from the Debye–Scherer formula is 10.59 nm.

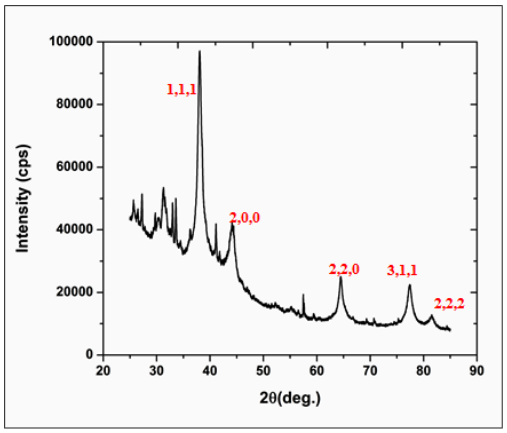

Fig.2 XRD image of biosynthesized Silver Nanoparticles

Five peaks at 2Θ values of 38.06, 44.16, 64.43, 77.33 and 81.38 deg corresponding to (111), (200), (220), (311) and (222) planes of Silver is observed and compared with the standard powder diffraction card of Joint Committee on Powder Diffraction Standards (JCPDS), silver file No. 04–0783. The XRD study suggests that the resultant particles are (FCC) SNP[21].

Table.1: Peak indexing from d–spacing of XRD of silver nanoparticles

2Ɵ	d (ang.)	$1000/d^2$	$(1000/d^2)/60.62$	hkl
38.06	2.36	179.54	2.96	111
44.16	2.05	237.95	3.925	200
64.43	1.44	482.25	7.955	220
77.33	1.23	660.98	10.90	311
81.38	1.18	718.18	11.85	222

The FCC crystal structure of silver has unit cell edge '*a'* = 4.07 Å and this value is calculated theoretically by using formula,

$$a = \frac{4}{\sqrt{2}} \times r \quad \text{.....} \quad (1)$$

For silver r =144 pm. The experimental lattice constant '*a*' is calculated from the most intense peak (111) of the XRD pattern is 4.087 Å.

Table.2: The size and lattice parameter of Silver nanoparticles

2Ɵ	hkl	FWHM(β) degree	FWHM(β) radian	D [size](nm)	d [spacing](nm)	a, lattice parameter (Å)
38.06	111	0.7924	0.0138	11.0	0.236	4.087
44.16	200	0.8477	0.0148	10.5	0.205	4.1
64.43	220	0.7136	0.0124	13.7	0.144	4.073
77.33	311	0.8915	0.0155	11.9	0.123	4.079
81.38	222	0.9314	0.0162	11.7	0.118	4.088

Both theoretical and experimental lattice constant '*a*' are in very well agreement. The lattice constant '*a*' details have been produced in Table.2 and the values in agreement with the literature report (*a* = 4.086 Å, JCPDS file no. 04-0783).

Particle Size Calculation

Average particle size has been calculated by using Debye-Scherrer formula[22, 23].

$$D = \frac{0.9\lambda}{\beta \cos\theta} \quad \text{.....} \quad (2)$$

Where 'λ' is wave length of X-Ray (0.1541 nm), 'β' is FWHM (full width at half maximum), 'Ɵ' is the diffraction angle and 'D' is particle diameter size. The calculated particle size details are in Table.2. The value of d (the interplanar spacing between the atoms) is calculated using Bragg's Law[24].

$$2dSin\theta = n\lambda \quad \text{.....} \quad (3)$$

Dislocation Density

The dislocation density is the length of dislocation lines per unit volume of the crystal. Dislocation is a crystallographic defect or irregularity, within a crystal structure in materials science. The presence of dislocations strongly determines many of the properties of materials. The dislocation density rises with plastic deformation. Three mechanisms for dislocation formation are formed by homogeneous nucleation, grain boundary initiation, and interface of the lattice and the surface precipitates, dispersed phases, or reinforcing fibers. A larger dislocation density implies a larger hardness. Chen and Hendrickson measured and determined dislocation density and hardness of several silver crystals and observed that crystals with larger dislocation density were harder[25]. It has been demonstrated for different pure face-centered cubic (FCC) metals processed by Equal Channel Angular Pressing (ECAP) that the decrease of grain size with increases of strains the dislocation density increases[26]. It is well known that above a certain grain size limit (~20 nm) the strength of materials increases with decreasing grain size[27, 28]. The average dislocation density of silver is ~$15 \pm 2 \times 10^{14}$ m^{-2}

as found from the analysis of X-ray line profiles[29,30].The dislocation density (δ) in the sample has been calculated using following expression[31].

$$\partial = \frac{15\beta Cos\theta}{4aD} \quad \ldots\ldots\ldots\ldots\ldots\ldots\ldots\ldots\ldots\ldots\ldots \text{(4)}$$

Where δ is dislocation density, β is broadening of diffraction line measured at half of its maximum intensity (in radian), ϴ is Bragg's diffraction angle (in degree), *a* is lattice constant (in nm) and *D* is particle size (in nm). The dislocation density of sample SNP found to be as 10.5×10^{14} m^{-2}.

Crystallinity Index

Peak breadth of a specific phase of material is directly proportional to the mean crystallite size of that material. Quantitatively, sharper XRD peaks are typically indicative of larger crystallite materials. From our XRD data, a peak broadening of the nanoparticles is noticed. The average particle size, as determined using the Scherrer equation, is calculated to be 10.59 nm. Crystallinity is evaluated through comparison of crystallite size as determined by TEM particle size determination[16]. Crystallinity index Eq. is presented below:

$$I_{Cry} = \frac{D_P(SEM,TEM)}{D_{Cry}(XRD)} (I_{Cry} \geq 1.00) \ldots\ldots\text{(5)}$$

Where Icry is the crystallinity index; Dp is the particle size (obtained from either TEM or SEM morphological analysis); Dcry is the particle size (calculated from the Scherrer equation). Result indicates the crystallinity index of the sample has found higher than 1.0. The data indicate that the silver metal is highly crystalline and FCC phase structure is well-indexed. If Icry value is close to 1, then it is assumed that the crystallite size represents monocrystalline whereas a polycrystalline have a much larger crystallinity index[32].

XRD - Specific Surface Area

Specific surface area (SSA) is a material property. The surface state will play an important role in the nanoparticles, due to their large surface to volume ratio with a decrease in particle size. It is a derived scientific value that can be used to find out the type and properties of a material. It has a particular importance in case of adsorption, heterogeneous catalysis and reactions on surfaces. SSA is the Surface Area (SA) per mass. Here V_{part} is particle volume and SA_{part} is particle SA[33].

$$SSA = \frac{SA_{Part}}{V_{Part} \times density} \ldots\ldots\ldots\ldots\ldots\ldots\ldots\ldots \text{(6)}$$

$$S = \frac{6\times10^3}{D_p\rho} \ldots\ldots\ldots\ldots\ldots\ldots\ldots\ldots\ldots\ldots \text{(7)}$$

Where S is the specific surface area, Dp is the size of the particles, and ρ is the density of silver 10.5 g/cm^3 [34]. Mathematically, SSA can be calculated using these formulas. Both of these formulas yield same result. Calculated value of SSA of the prepared SNP is 53.96 m^2/g.

Scanning electron Microscopy

Scanning electron microscopy (SEM) analysis shows roughly spherical shape uniformly distributed SNP on the surfaces of the cells (Figure- 4). The size of the SNP was in the particle size ranges of 10-30 nm.

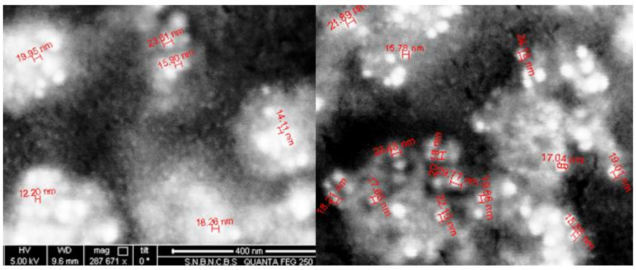

Fig. 3 FESEM micrograph of biosynthesized silver nanoparticles

Antibacterial action

Biologically synthesized silver nanoparticles are found toxic against Gram negative and Gram positive bacteria at a concentration of 100µM (Fig. 4). The antimicrobial properties of silver compounds and silver ions had been historically recognized and applied in a wide range of applications from disinfecting medical devices and home appliances to water treatment. Silver nanoparticles exhibited antibacterial activity against *E. coli, and S. aureus* as it showed a clear inhibition zone of SNP along with standard antibiotics streptomycin, and silver salt solution (Table 3).

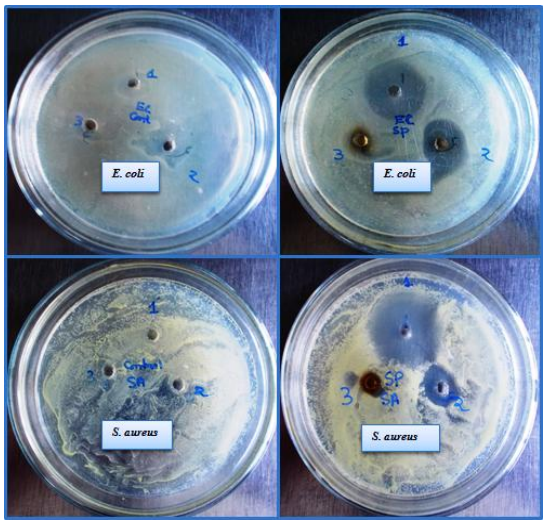

Fig.4 Antibacterial effect of silver nanoparticles against *E. coli, and S. aureus* (1-streptomycin, 2-silver nitrate, 3-silver nanoparticles).

Table 3: Zone of inhibition of antibacterial activity

Microbial Strain	Zone of Inhibition (in mm)		
	Streptomycin (1)	Silver Nitrate (2)	Silver Nanoparticles (3)
E. coli	20	18	9
S. aureus	26	16	11

From the growth kinetics of both Gram negative and Gram positive bacteria it has been observed that the growth of both strain initially inhibited in presence of SNP and after incubation of 2h similar type of growth has been noticed. From the growth curve it was clear that growth of both Gram negative and Gram positive bacteria suppressed in presence of SNP.

Conclusion

XRD studies reveal that biologically prepared SNP are face-centered cubic (FCC) crystal with a high degree of crystallinity and monophasic SNP. XRD has also analyzed their various characters like specific surface area, and dislocation density. FESEM images show spherical shape 10-30 nm size SNP. Siver nanoparticles show zones of inhibition against the growth of both *E. coli*, and *S. aureus*. Thus it is proven from this study that the SNP synthesized from *Aspergillus foetidus* seems to be promising and effective antibacterial agent against the Gram negative and Gram positive strains of bacteria.

Acknowledgement:

Swarup Roy is thankful to the Department of Science Technology (New Delhi, India) for his DST INSPIRE fellowship.

References :

1. Tolaymat T, Badawy El, Genaidy A, Scheckel A, Luxton KT, and Suidan., An evidence-based environmental perspective of manufactured silver nanoparticle in syntheses and applications: a systematic review and critical appraisal of peer-reviewed scientific paper, M. Sci. Tot. Environ., 2010, 408, 999-1006.
2. Chen JC, Lin ZH, and Ma XX., Evidence of the production of silver nanoparticles via pretreatment of *Phoma* sp 32883 with silver nitrate, Letters in Applied Microbiology, 2003, 37, 105–108.
3. Shaligram NS, Bule M, Bhambure RM, Singhal RS, Singh SK, and Szakacs G., Biosynthesis of silver nanoparticles using aqueous extract from the compactin producing fungal strain, Process Biochemistry, 2009, 44, 939–948.
4. Jha AK, Prasad K, Prasad K, and Kulkarni AR., Plant system: nature's nanofactory, Colloids and Surfaces B: Biointerfaces, 2009, 73, 219–223.
5. Mubarak AD, Sasikala M, Gunasekaran M, and Thajuddin N., Biosynthesis An Characterization Of Silver Nanoparticles Using Marine Cyanobacterium, *Oscillatoria Willei* Ntdm01, Digest Journal of Nanomaterials and Biostructures, 2011, 6, 385-390.
6. Rai M, Yadav A, and Gade A., Silver nanoparticles as a new generation of antimicrobials, Biotechnology Advances, 2009, 27, 76–83.
7. Duran N, Marcato PD, Alves OL, DeSouza G, and Esposito E., Mechanistic aspects of biosynthesis of silver nanoparticles by several *Fusarium oxysporum* strains, Journal of Nanobiotechnology, 2005, 3, 1-8.
8. Ingle A, Gade A, Pierrat S, Sonnichsen C, and Rai MK., Mycosynthesis of silver nanoparticles using the fungus *Fusarium acuminatum* and its activity against some human pathogenic bacteria, Current Nanoscience, 2008, 4, 141–144.
9. Kim JS, Kuk E, Yu KN, Kim JH, Park SJ, Lee HJ, Kim SH, Park YK, Park YH, Hwang CY, Kim YK, Lee YS, Jeong DH, and Cho MH., Antimicrobial effects of silver nanoparticles, Nanomed: Nanotechnol Biol Med., 2007, 3, 95–101.
10. Kim KJ, Sung WS, Suh BK, Moon SK, Choi JS, Kim JG, and Lee DG., Antifungal activity and mode of action of silver nano-particles on Candida albicans, Biometals: Int J Role Metal Ions Biol Biochem Med., 2009, 22, 235–242.
11. Asharani PV, Hande MP, and Valiyaveettil S., Anti-proliferative activity of silver nanoparticles, BMC Cell Biol., 2009, 10, 1-14.
12. Morones JR, Elechiguerra JL, Camacho A, and Ramirez JT., The bactericidal effect of silver nanoparticles, Nanotechnol., 2005, 1, 2346-2353.
13. Albrecht MA, Evan CW, and Raston CR., Green chemistry and the health implications of nanoparticles. Green Chem., 2006, 8, 417-432.
14. Baker C, Pradhan A, Paktis L, Pochan DJ, and Shah SI., Synthesis and antibacterial properties of silver nanoparticles, J. Nanosci. Nanotechnol., 2005, 5, 244-249.
15. Martinez- Castanon GA, Nino- Martinez N, Martinez-Gutierrez F, JR Martinez Mendoza JR, and Ruiz F., Synthesis and antibacterial activity of silver nanoparticles with different sizes, J. Nanopart Res., 2008, 10, 1343-1348.
16. Roy S, Mukherjee T, Chakraborty S, and Das TK., Biosynthesis, characterisation & antifungal activity of Silver nanoparticles synthesized by the fungus *Aspergillus foetidus* MTCC8876, Digest J. Nanomater. Biostruct., 2013, 8, 197-205.
17. Roy S, and Das TK., Synthesis and standardization of biologically synthesized silver nanoparticles, AIP Proc., 2013, 1536, 39-40.
18. Roy S, and Das TK., Biosynthesis of Silver Nanoparticles by *Aspergillus foetidus*: Optimization of Physicochemical Parameters, Nanosci. Nanotechnol. Lett., 2014, 6, 181-189.
19. Roy S, and Das TK., Activity of Biosynthesized Silver Nanoparticles in Combination with Synthetic and Natural Fungicide Against some Pathogenic Fungi, Asian J Chem., 2013, 25, s315-317.
20. Wani IA, Ganguly A, Ahmed J, and Ahmad T., Silver nanoparticles: ultrasonic wave assisted synthesis, optical characterization and surface area studies, Mat. Lett., 2011, 65, 520-522.
21. Lanje AS, Sharma SJ, and Pode RB., Synthesis of silver nanoparticles: a safer alternative to conventional antimicrobial and antibacterial agents, J. Chem. Pharm. Res., 2010, 2, 478-483.
22. Cullity B.D., Elements of X-ray Diffraction, Addison-Wesley Company, USA (1956).
23. John R, and Florence SS., Structural and Optical properties of ZnS nanoparticles synthesized by solid state reaction method, Chalcogenide Lett., 2009, 6, 535-539.
24. Theivasanthi T, and Alagar M., X-Ray Diffraction Studies of Copper Nanopowder, Archives of Physics

Research, 2010, 1, 112-117.
25. Sirdeshmukh DB, Sirdeshmukh L, and Subhadra KG., Micro- and Macro-Properties of solids: Thermal, Mechanical and Dielectric properties, Springer, New York (2006).
26. Chinh NQ, Gubicza J, and Langdon TG., Review Characteristics of Face-Centered Cubic Metals Processed by Equal-Channel Angular Pressing, J. Mater. Sci., 2007, 42, 1594-1605.
27. Weertman JR., Hall–Petch strengthening in nanocrystalline metals, Mater. Mater. Sci. Eng. A, 1993, 166, 161-167.
28. Van Swygenhoven H., Grain boundaries and dislocations, Science, 2002, 296, 66-67.
29. Gubicza J, Chinh NQ, Labar JL, Hegedus Z, Szommer P, Tichy G, and Langdon TG., Delayed microstructural recovery in silver processed by equal-channel angular pressing, J. Mater. Sci., 2008, 43, 5672-5676.
30. Majeed Khan MA, Kumar S, Ahamed M, Alrokayan SA, and AlSalhi MS., Structural and thermal studies of silver nanoparticles and electrical transport study of their thin films, Nanoscale Res.Lett., 2011, 6, 1-8.
31. Venkata Subbaiah YP, Prathap P, and Ramakrishna Reddy KT., Structural, electrical and optical properties of ZnS films deposited by close-spaced evaporation, Appl. Surf. Sci., 2006, 253, 2409-2415.
32. Pan X, Medina-Ramirez I, Mernaugh R, and Liu J., Nano characterization and Bactericidal Performance of Silver Modified Titania Photocatalyst, Colloids and Surfaces B: Biointerfaces, 2010, 77, 82-89.
33. Antony J, Nutting J, R. Baer D, Meyer D, Sharma A, and Qiang Y., Size-dependent specific surface area of nanoporous film assembled by core-shell iron nanoclusters, Journal of Nanomaterials, 2006, 54961, 1-4.
34. Park J-Y, Lee Y-J, Jun K-W, Baeg J-O, and Yim DJ., Chemical synthesis and characterization of highly oil dispersed MgO nanoparticles, J. Ind. Eng. Chem., 2006, 12, 882-887.

*****